

LINKING MICROSTRUCTURE AND HIGH TEMPERATURE DUCTILITY IN ALUMINIUM ALLOYS AA6XXX

Lassance D., Schmitz M., Delannay F. and Pardoën T.

Département des sciences des Matériaux, Université catholique de Louvain, PCIM.

2, Place Sainte Barbe, B-1348 Louvain-La-Neuve, Belgium.

lassance@pcim.ucl.ac.be

Abstract

The link between the hot deformation damage behaviour of two aluminium alloys AA6xxx and the microstructural evolution occurring during the homogenisation treatment is studied in order to improve the understanding and the control of the damage resistance during extrusion. The hot ductility and deformability of these alloys were investigated from a campaign of uniaxial tension tests on smooth and notched cylindrical rods by varying the deformation temperature, second phase particles content and stress state. Large β -AlFeSi particles impair hot ductility by a mechanism of nucleation, growth and coalescence around the brittle particles. A higher homogenisation temperature and soaking time is shown to improve the transformation of the brittle platelike monoclinic β -AlFeSi particles to the more rounded cubic α -AlFeSi particles, which results in superior hot deformability and ductility. Finite elements model simulations based on an enhanced version of the Gurson void growth model is used to more quantitatively relate microstructure and ductility.

Introduction

It is well known that homogenised aluminium alloys billets extrude easier and faster and give a better surface finish than as-cast billets. Structural aluminium alloys contain inclusions of brittle phase dispersed in a ductile matrix. Damage initiation occurs in such alloys by decohesion or fracture of these inclusions as referred by Agarwal *et al.* [1], Bae and Ghosh [2], Balasundaram *et al.* [3] and Toda and Kobayashi [4]. The resistance to failure depends directly on the second phase particle content. These particles can be several microns large, and do not contribute to strengthening. They are easily observed at grain boundaries. The Fe-bearing intermetallic particles such as β -Al₃FeSi and α -Al₁₂(Fe,Mn)₃Si have a significant influence on formability. Their morphology and nature vary depending on chemistry and thermal treatments. The brittle plate-like monoclinic β phase is associated to poor hot workability. This unfavourable effect can be improved by performing a long homogenisation treatment at high temperature, by which the β phase transforms to the more rounded, metastable, cubic α phase.

The link between hot deformation damage behaviour of two aluminium alloys of the 6xxx family (AA6063 and AA6005A) and microstructural evolution during the homogenisation treatment is studied and compared with the behaviour at room temperature. The goal of this work is to improve the understanding and the control of the damage resistance during hot extrusion.

The microstructure evolution ($\beta \rightarrow \alpha$ transformation) is studied by energy dispersive X-ray analysis (EDS) coupled with scanning electron microscope (SEM). The accompanying morphology change is measured by image analysis. The hot ductility is investigated from a campaign of uniaxial tension tests on smooth and notched cylindrical rods at various

deformation temperatures with different second phase particles contents. Finite elements (FEM) simulations based on an enhanced micromechanics-based void growth model are used to more quantitatively relate microstructure and ductility.

Experimental

The alloys used in the present investigation were cast industrially. Their chemical composition are 0.49 Mg, 0.43 Si, 0.22 Fe, 0.02 Mn for alloy AA6063 and 0.56 Mg, 0.59 Si, 0.18 Fe, 0.04 Mn for alloy AA6005A. Homogenisation trials were performed by changing the soaking time and temperature. Soaking experiments were performed at 585°C and 600°C with a 30'-300' soak.

Homogenised samples were prepared with standard metallographic techniques: grinding with SiC paper, polishing with 9-6-3 μm diamond paste and finishing with colloidal silica. They were examined by a scanning electron microscope. An energy dispersive X-ray analyser (EDS) was used for identification and quantification of the intermetallic phases. Computer based image analysis was used for measuring the particle morphology change.

Cylindrical tensile specimens with a diameter of 9 mm and a gage length of 40 mm were machined from industrially homogenised 8" diameter billets. The stress state was varied by using notched specimens with notch radii of 2 mm and 5 mm. Tensile testing was performed on a screw-driven machine at a strain rate of 5 mm/min. The series of tests was performed at temperatures ranging between 20°C and 590°C.

Micromechanical model for void growth and coalescence

The model developed by Pardoen and Hutchinson [5] was used to obtain a theoretical prediction of the maximum ductility before fracture. The model is well suited for the present case as it incorporates void shape effects which is key to capture the impact of the $\beta \rightarrow \alpha$ transformation on the ductility. The void shape is here directly linked with the intermetallic particles aspect ratio. The void aspect ratio is defined as $W = R_z/R_r$. The dimensions of the representative void cell are defined in Fig. 1. A description of the model can be found in other papers [5].

In order to apply the void growth model, the material flow properties must be known as well as three microstructural parameters: (1) *the initial aspect ratio of the voids* W_0 , which will depend on the particles shape and on the damage initiation mode (which varied with deformation temperature); (2) *the initial void distribution* λ_0 , which will be assumed uniform; (3) *the initial void volume fraction* f_0 , which is related to the initial inclusions fraction. Void nucleation is assumed to occur at the beginning of straining.

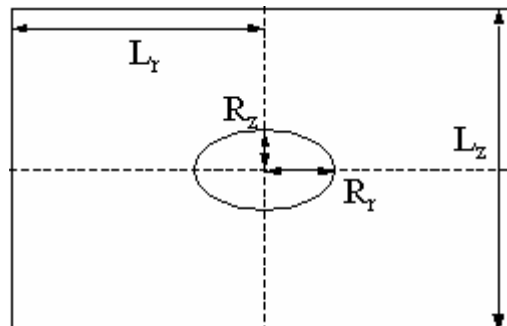


FIGURE 1. Representative volume element.

The initial parameters have been calibrated in the following way:

(a) We computed the necking deformation of a smooth tensile specimen to obtain an improved stress-strain curve representative of the response at large-deformation. Such a flow curve cannot be measured experimentally but may be obtained by simulating the test, matching all measurable quantities, and hence obtaining the correct stress-strain state by iteration, as reported for instance by Norris *et al.* [6].

(b) In a first series of simulation, we assumed that the intermetallic particles give rise to a void by decohesion for all deformation temperatures. We used as initial void volume fraction f_0 the intermetallic particles content, f_p , and we varied the initial aspect ratio of the voids W_0 in order to account for different homogenisation states.

Experimental Results

Microstructure evolution

As-cast samples of aluminium alloys AA6063 and AA6005A were homogenised at 585°C and 600°C for different periods of time. During this treatment, several processes take place, such as the transformation of interconnected plate-like monoclinic β -Al₅FeSi particles into more rounded discrete cubic α -Al₁₂(Fe,Mn)₃Si particles. The transformation rate was measured as well as the accompanying particle shape change, which is deemed to be the most important parameter for obtaining a good extrudability. The results are presented in Fig. 2. We can see the huge difference in kinetics of the $\beta \rightarrow \alpha$ transformation at 585°C and at 600°C.

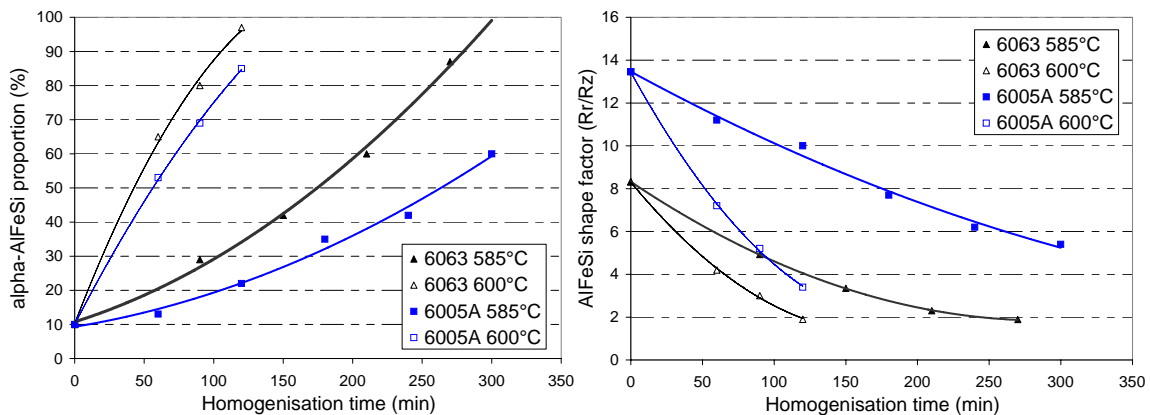


FIGURE 2. Evolution of the α -Al₁₂(Fe,Mn)₃Si particles proportion (%) and of the mean aspect ratio with the homogenization time.

Tensile tests

The hot ductility of the homogenised alloys was investigated at different temperatures by tensile testing. In Fig. 3, the logarithm of the reduction of area ($\ln(A_0/A_f)$) is plotted as a function of the deformation temperature for both alloys with different α contents. The reductions of area are very high, but decrease abruptly around 570-580°C for the AA6063 specimens, before they increase again at 590°C. The hot ductility profile was different for the alloy AA6005A, with a decrease in ductility above a certain threshold temperature. A significant difference in ductility was observed between the two alloys. Lower Si and Mg contents were found to have a beneficial effect on hot ductility. If we imagine that the

ductility of the alloy AA6063 will decrease after 590°C, its threshold temperature is higher and thus clearly influenced by the Si content presumably through its effect of stabilising the β phase against melting as reported by Zajac *et al.* [7].

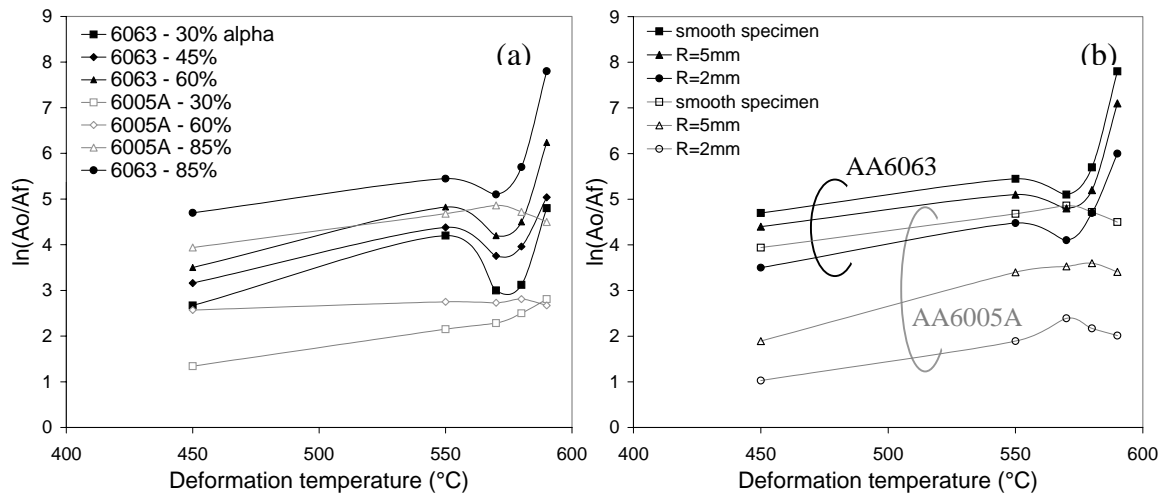


FIGURE 3. Evolution of the ductility with deformation temperature for differently homogenized smooth uniaxial tensile specimens of AA6063 and AA6005A (a) and for both alloys with 85% of alpha particles for different notched specimens (b).

An effort has been made to elucidate the origin of the changes in hot ductility of the alloy AA6063. The fracture surface of tensile specimens was analysed by SEM/EDS. The results are shown in Fig. 4 for the alloy containing 60% of α -AlFeMnSi particles. The observations revealed that the fracture was ductile up to 550°C. Large particles were present on the fracture surfaces. It is evident from the microstructural observations that these particles are brittle β -Al₃FeSi phase and act as crack nuclei. They also contribute to intergranular decohesion. However, the fracture surfaces are different for the specimens deformed at 570°C and 580°C. Indeed, in the latter case we observed intergranular and shear like fracture surfaces without dimples. This can be related to the observed fall in ductility at this temperature. This fracture mechanism is typical of fracture due to incipient melting inside an alloy. This result corresponds to the observation previously made with this alloy by Lassance *et al.* [8]. Indeed, in the studied alloy AA6063, we observed the presence of pure silicon inclusions combined with the presence of β -Al₃FeSi particles. This microstructure was identified by DSC measurements which show evidence of the eutectic melting reaction $\text{Al} + \beta\text{-Al}_3\text{FeSi} + \text{Si} \rightarrow \text{liquid}$, at 578°C. This reaction appears thus responsible for the fall in ductility observed at these temperatures.

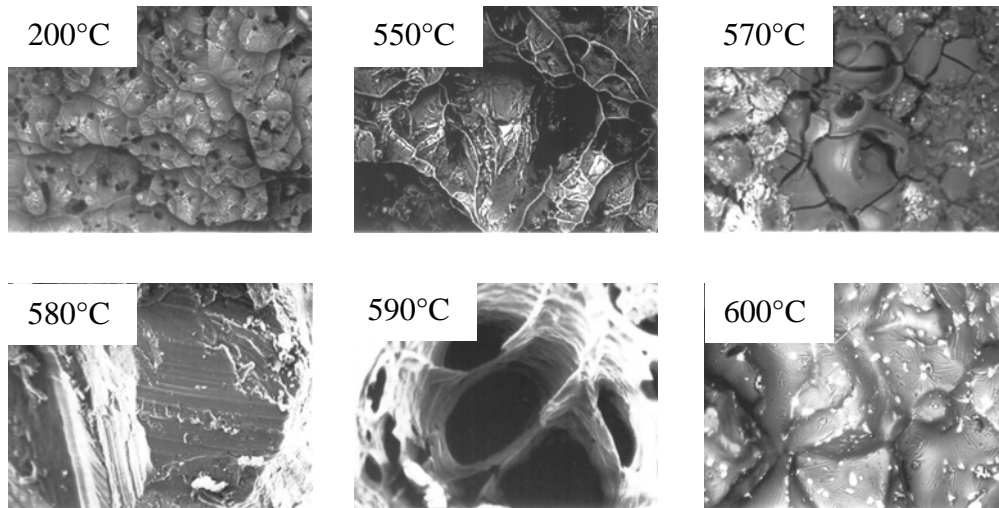


FIGURE 4. SEM micrographs of fracture surfaces of AA 6063 alloy loaded under tensile testing from 200°C to 600°C.

At 590°C, the fracture is again ductile. Only some big and very deep dimples were then observed on the fracture surface. Finally, the fracture surface at 600°C showed evidence of melting.

The results for the notched tensile tests are summarized in Fig. 4 and compared with the smooth specimen results. The same behavior is observed when the deformation temperature increases whereas a triaxiality increase causes a decrease of ductility.

Elasto-plastic finite-element simulation of the uniaxial tensile test

Tensile tests were simulated by FEM calculations using the commercial software Abaqus. A user defined material subroutine implementing the extended Gurson model was used for modelling ductile fracture. Controlled displacement simulations are carried out in order to predict the *cross-section area at fracture (A_f)* for the two alloys, the AlFeSi particle aspect ratio (W_0) and the deformation temperature. The experimental uniaxial stress-strain curves of the AA6063 and AA6005A alloys extrapolated to large strains were used as the flow properties in the FE model to simulate the elasto-plastic response.

In this series of simulation, we assumed that the intermetallic particles give rise to a void by decohesion for all deformation temperatures. We used as initial void volume fraction f_0 the intermetallic particles content, f_p , and we varied the initial aspect ratio of the voids W_0 in order to account for different homogenisation state. We used two different initial void volume fraction equal to $f_0 = \gamma f_p$ with $\gamma = 1$ and 0.1.

Linking the experimental relationship between the particles aspect ratio and the homogenisation conditions with the relationship between the ductility and the particles aspect ratio given by modelling, we obtained a relationship between the maximum ductility at fracture in tension and the homogenisation conditions. These results are shown in Figs 5 and 6.

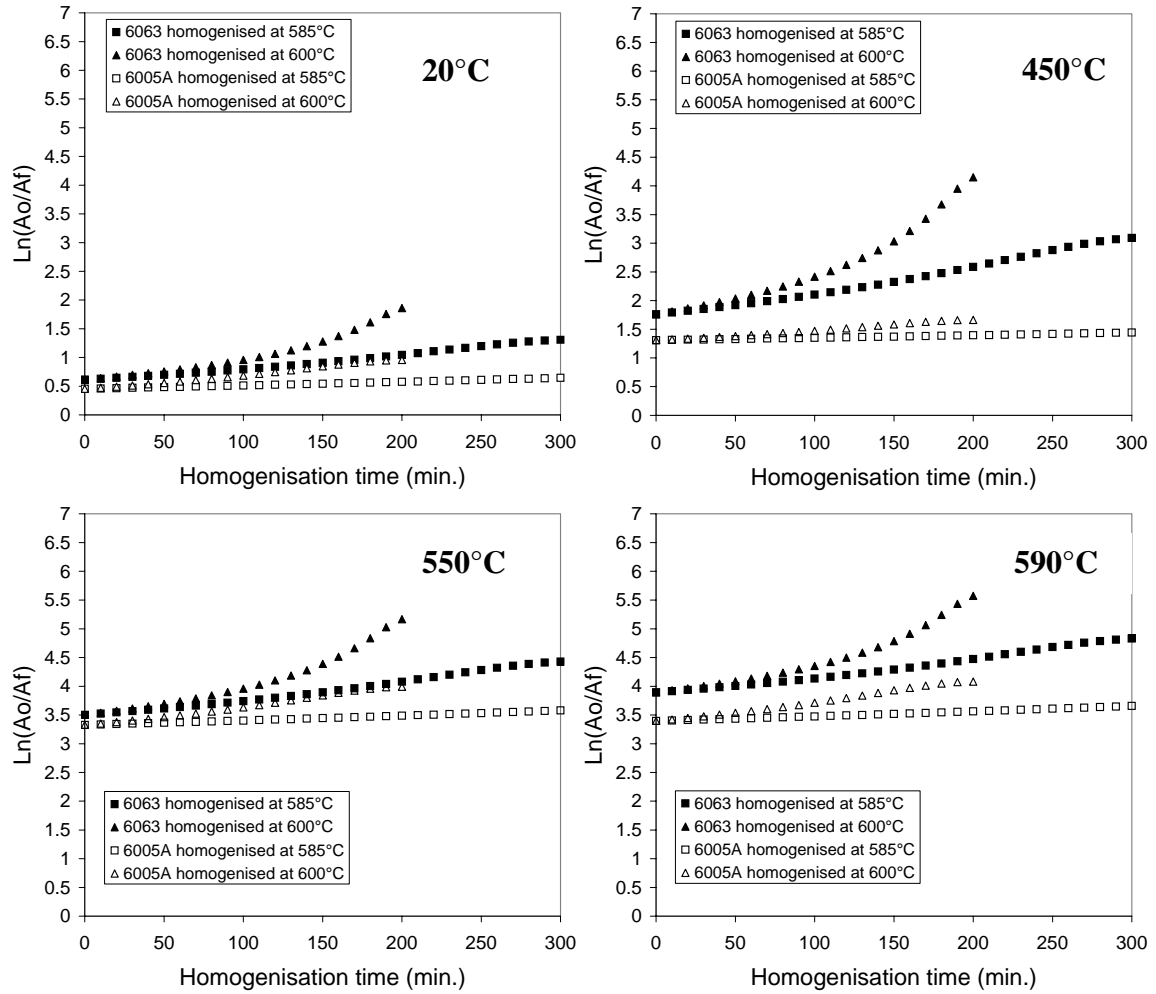


FIGURE 5. Relationship between the ductility ($\ln(A_o/A_f)$) and the homogenization conditions at 20°C (a), 450°C (b), 550°C (c) and 590°C (d) for the aluminium alloys AA6063 and AA6005A with $\gamma = 1$.

Compared to the experimental results, the FEM simulations with $f_o = f_p$ predict a maximum ductility which is too high especially at room temperature and for the alloy AA6005A. Nevertheless, above 450°C, the results are good for the alloy AA6063. Concerning the alloy AA6005A, we can conclude that either the damage mechanism is different, or only some intermetallic particles play a part in the damage initiation. The calculations made with $f_o = 0.1 f_p$ give indeed results which are more close to the experimentally measured ductility for the more alloyed material.

The parameters used in the model have been defined accounting only for particle/matrix decohesion. We have indeed taken the initial void aspect ratio equal to the particle aspect ratio. At low temperature, the results can be influenced by the fact that particles oriented in the tension direction will probably cracked and induced different initial void fraction and different initial void aspect ratio. We will account for this information in a next study.

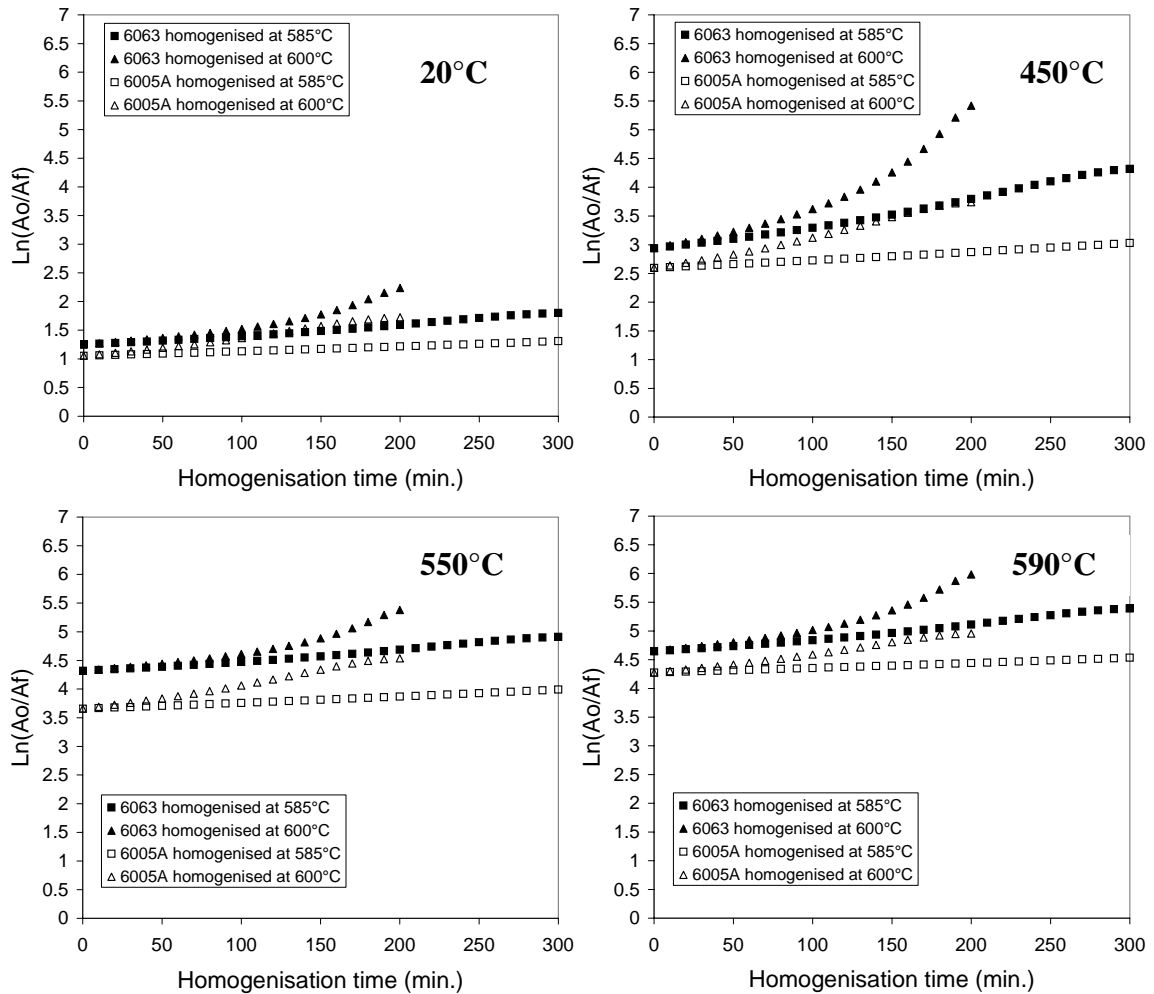


FIGURE 6. Relationship between the ductility ($\ln(A_0/A_f)$) and the homogenization conditions at 20°C (a), 450°C (b), 550°C (c) and 590°C (d) for the aluminium alloys AA6063 and AA6005A with $\gamma = 0.1$.

Discussion

During deformation, the metal temperature increases owing to the deformation and friction in the press. The maximum extrusion speed is usually limited by the hot cracking temperature, which may be associated to the embrittling effect of second phase particles or to the melting caused by eutectic reactions. It usually coincides with the appearance of broken particles on the fracture surface. The present work has firstly demonstrated that the $\beta \rightarrow \alpha$ transformation during the homogenisation heat treatment depends on the chemical composition. In the alloy AA6063 with lower Si and Mg content, the transformation occurs fairly rapidly and depends mainly on homogenisation temperature. However, at a higher Si content (alloy AA6005A), the transformation process is very slow and implies a temperature of 600°C to accelerate the transformation. This work has also shown a distinct transition in mechanical behaviour during high temperature deformation, which is dependent on the composition and second phase particles content (and aspect ratio). In the alloy AA6063, a first transition in mechanical behaviour around 570-580°C has been shown to be caused by incipient melting due to the eutectic reaction $\text{Al} + \beta\text{-Al}_3\text{FeSi} + \text{Si} \rightarrow \text{liquid}$, at 578°C. This is probably related to the presence of pure Si resulting from the casting process. The other transition in

mechanical behaviour at higher temperature can be shown to occur under conditions where the rates of dislocation accumulation and annihilation in the vicinity of particles are equal [8].

Finally, the FEM simulations allowed to directly relate the maximum ductility (at fracture) with the homogenisation heat treatment parameters. These results give us information about the difference in ductility between alloys AA6063 and the AA6005A. It gives us also an idea of the saving of time obtained by increasing the homogenisation temperature above 585°C. This temperature is rarely exceeded because of the eutectic melting of the Mg₂Si phase at 585°C, whereas the latter precipitates are dissolved during the very first stage of the homogenisation (during the heating to the homogenisation temperature).

In a next study, we will investigate the influence of the deformation temperature and of the composition on the damage initiation modes in order to use more accurate parameters in the simulations. This will be done by in situ and interrupted tensile testing.

Acknowledgements

The support of the Région Wallonne through a « Subvention Entreprise » (contract # 4436) with Sapa RC profile, Ghlin, Belgium, is gratefully acknowledged. D. Lassance acknowledges also Sapa RC Profile for the supply of material and for the homogenisation heat treatments.

References

1. Agarwal, H., Gokhale, A.M., Grahnam, S. and Horstemeyer, M.F., *Met. and Mat. Trans. A*, Vol. 33A, 2599-2606, 2002.
2. Bae, D.H. and Ghosh, A.K., *Acta Materialia*, Vol. 50, 511-523, 2002.
3. Balasundaram, A., Gokhale, A.M., Graham, S. and Horstemeyer, M.F., *Mat. Sc. and Eng. A*, Vol. 355, 368-383, 2003.
4. Toda, H. and Kobayashi, T., *Mat. Sc. Forum*, Vols 426-432, 393-398, 2003.
5. Pardoën, T. and Hutchinson, J.W., *J. Mech. and Phys. of Sol.*, Vol. 48, Issue 12, 2467-2512, 1998.
6. Norris, D.M., Moran, B., Scudder, J.K. and Quinones, D.F., *J. Mech. Phys. Solids*, Vol. 26, 1-19, 1978.
7. Zajac, S., Hutchinson, B., Johansson, A. and Gullman, L.-O., *Mat. Sc. and Tech.*, Vol. 10, 323-333, 1994.
8. Lassance, D., Dille, J., Delplancke, J.L., Pardoën, T., Ryelandt, L. and Delannay, F., *Mat. Sc. Forum*, Vols 426-432, 447-452, 2003.